The Farnesyltransferase Inhibitor R115777 Reduces Hypoxia and Matrix Metalloproteinase 2 Expression in Human Glioma Xenograft

Caroline Delmas,[1] Dave End,[2] Philippe Rochaix,[3] Gilles Favre,[1] Christine Toulas,[1] and Elizabeth Cohen-Jonathan[1,4]

[1]Laboratoire d'Oncologie Cellulaire et Moléculaire Institut National de la Santé et de la Recherche Médicale U593, Institut Claudius Regaud, Toulouse Cedex, France; [2]Johnson & Johnson Pharmaceutical Research & Development, Titusville, New Jersey; [3]Laboratoire d'Anatomo-pathologie, Institut Claudius Regaud, Toulouse Cedex, France; and [4]Département de Radiothérapie, Institut Claudius Regaud, Toulouse Cedex, France

ABSTRACT

Purpose: **The high-grade primary brain tumors, glioblastoma, of extremely bad prognosis contain large regions of hypoxia known to be involved in the chemo- and radioresistance. We demonstrated previously that radioresistant human wild-type Ras U87 glioblastoma can be radiosensitized *in vitro* by the specific farnesyltransferase inhibitor R115777. The aim of this study was to analyze the effect of this compound on the hypoxic status and the vascularization of this tumor.**

Experimental Design: **U87 xenografts bearing mice were treated with 100 mg/kg of R115777 bid during 4 days. Hypoxia was assessed by measuring the binding of hypoxic cell marker pentafluorinated 2-nitroimidazole. Immunohistochemistry was performed to analyze angiogenesis and metalloproteinase-2 expression.**

Results: **We demonstrated here that R115777 treatment induced a significant oxygenation of U87 xenografts ($P < 0.001$) associated with a decrease of hypoxia-inducible factor 1α expression. This reduction of hypoxia was not due to a decrease of tumor size after R115777 treatment. This oxygenation was associated with a change in vessel morphology and with a significant decrease of the vessel density. Moreover, R115777 treatment reduced matrix metalloproteinase 2 expression in xenografts and inhibited matrix metalloproteinase 2 activity *in vitro*. These data strongly suggest that R115777 could increase this tumor oxygenation at least by interacting with angiogenesis.**

Conclusion: **Our results demonstrate that R115777 treatment inhibits different pathways leading to the radioresistance of wild-type Ras expressing glioblastoma, including intrinsic radioresistance, hypoxia, and angiogenesis. These combined effects on glioblastoma underline the interest of associating R115777 with radiotherapy as a new treatment of these tumors of catastrophic prognosis.**

INTRODUCTION

The high-grade primary brain tumors, glioblastoma, of extremely bad prognosis despite surgery, radiotherapy, and chemotherapy, are known to contain large regions of hypoxia. The presence of these hypoxic regions is associated with a more malignant tumor phenotype. These regions are resistant to the different therapies used in clinical oncology, especially radiotherapy, resulting in a worse prognosis (1–5). These data strongly suggest that tumor hypoxia could be an important therapeutic target.

The FTIs[5] were initially synthesized to block the Ras oncogenic processing by inhibiting the addition of a prenyl side chain by farnesyltransferase, which is a requirement for Ras activity (6–9). Several works have implicated Ras in radioresistant phenotype (10–12). Bernhard *et al.* (13) have shown that FTI treatment radiosensitizes H-ras-transformed rat embryo fibroblasts and human tumor cell lines expressing activated H-ras *in vitro* (14). We have demonstrated a radiosensitization of tumors with mutated H-Ras by FTI *in vivo* (12) and additionally shown that part of this *in vivo* effect was due to a reduction of hypoxia in tumors expressing H-ras mutation (15). However, the FTI radiosensitizer effect is not limited to mutated Ras-expressing tumors. We have shown recently that the treatment of radioresistant HeLa cells transfected by the cDNA encoding for the M_r 24,000 isoform of the FGF-2 with FTI-277 induces a radiosensitization, whereas these cells do not express a mutated H-Ras (16). The same radiosensitizer effect was observed in the radioresistant human U87 glioblastoma cell line that express wild-type Ras and FGF-2 after treatment with the specific FTI R115777 (17). Moreover, we have shown in these two cellular models that Ras was not involved in the control of the radioresistance pathway (18, 19). Taken together, these different data suggested that FTI could modify the microenvironment in tu-

Received 4/24/03; revised 8/14/03; accepted 8/15/03.
Grant support: Ministere de la Recherche et de l'Enseignement Supérieur (G. F, E. C. J.), by the Groupe de Recherche de l'Institut Claudius Regaud (C. T., E. C. J.), and by Electricité de France.
The costs of publication of this article were defrayed in part by the payment of page charges. This article must therefore be hereby marked *advertisement* in accordance with 18 U.S.C. Section 1734 solely to indicate this fact.
Note: Dave End is employed by the Janssen Research Foundation, a wholly owned subsidiary of Johnson and Johnson Pharmaceutical Research and Development (J&J PRD) and holds significant stock in J&J.
Requests for reprints: Elizabeth Cohen-Jonathan-Moyal, Dpt de Radiothérapie, Institut Claudius Regaud 20–24 rue du Pont St Pierre, 31052 Toulouse Cedex, France. Phone: 33-5-61-42-41-78; Fax: 33-5-61-42-46-43; E-mail: moyal@icr.fnclcc.fr.

[5] The abbreviations used are: FTI farnesyltransferase inhibitor; FGF, fibroblast growth factor; EF5, pentafluorinated 2-nitroimidazole; HIF, hypoxia-inducible factor; VEGF, vascular endothelial growth factor.

mors that are radiosensitized by this class of compound, and express wild-type Ras and FGF-2. The purpose of this study was to examine the effect of R115777 treatment on hypoxia status and angiogenesis of human radioresistant U87 glioblastoma xenografts implanted in mice.

MATERIALS AND METHODS

Cell Culture. Human glioblastoma U87 cells were routinely maintained in DMEM supplemented with 10% calf serum at 37°C in 5% CO_2-humidified incubators and subcultured weekly. Hypoxic conditions were obtained incubating U87 cells in a sealed "Bug-Box" anaerobic workstation (Ruskinn Technologies, Leeds, United Kingdom/Jouan, St. Herblain, France). The oxygen in the workstation is maintained at 1% with the residual gas mixture being 94% nitrogen and 5% carbon dioxide.

Tumor Xenograft Generation. Pathogen-free NMRi *nu/nu* mice (Janvier, Le Genest-St-L'Isle, France) were housed aseptically. At 5–7 weeks of age, mice were inoculated by s.c. injection into the hind flank with 1×10^6 U87 cells resuspended in serum-free DMEM. Once the U87 xenografts generated, mice were treated with R115777 delivered by gavage at a concentration of 100 mg/kg bid in 20% β hydroxypropyl cyclodextrine (Sigma, St. Quentin Fallavier, France) diluted in HCl 0.1 N, during 4 days.

Analysis of Farnesylation Inhibition by R115777. Tumor xenografts treated or not with R115777 (Johnson and Johnson Pharmaceutical Research, Spring House, PA) were lysed by Polytron (Luzern, Switzerland). Cells were harvested from monolayer cultures by rinsing with cold PBS twice, followed by scraping with a rubber policeman. Tumor extracts or cells were then incubated on ice in iced 50 mM Tris (pH 8.0), 1 mM EDTA, 250 mM NaCl, 0.5% (v/v) Triton X-100, 10 mM sodium orthovanadate, 50 mM sodium fluoride, 10 mM paranitrophenylphosphate, 1 mM dithiothreitol, 1 mM phenylmethylsulfonyl fluoride, and 1 μg/ml of leupeptin and pepstatine followed by incubation for 30 min on ice. After centrifugation at 10,000 rpm for 10 min at 4°C, protein concentration was quantified in the supernatant. Proteins (40 μg) were separated on 12% SDS-PAGE. The proteins were then transferred to nitrocellulose (0.22 μm) under 250mA for 1 h. Blots were blocked with TBST buffer [10 mM Tris (pH 8.0), 150 mM NaCl, and 0.1% Tween 20] containing 5% of nonfat dried milk protein for 1 h at room temperature, then probed with a rabbit polyclonal anti-Ha Ras antibody (Santa-Cruz Technology, Santa Cruz, CA; 1:1,000) or a monoclonal HDJ-2 antibody (Neomarker, Montlucon, France; 1:10,000) overnight at 4°C, washed three times for 10 min at room temperature with TBST. For staining of the protein bands, horseradish peroxidase-labeled goat antirabbit IgG or antimouse IgG antibodies were respectively used at 1:10,000 and 1:5,000 dilutions in TBST containing 4% nonfat dried milk protein for 1 h at room temperature, then washed again three times with TBST. After incubation in the enhanced chemiluminescence system, the membranes were exposed to Hyperfilm MP.

EF5 Detection of Hypoxia and Vessels Detection. After completion of the 4 days of R115777 or vehicle administration, mice were injected with 10 mM EF5 in 0.9% saline i.v. (0.01 ml/g body weight), followed by an equal volume i.p. injection 30 min later. Tumors were then immediately frozen after sacrifice. Frozen tissue sections (5 μm) were cut from the tumor onto poly-L-lysine coated slides, fixed in 4% paraformaldehyde for 1 h, and then rinsed. For hypoxia detection, slides were stained after fixation and rinsing with Cy3-conjugated ELK-51 (75 μg/ml), a mouse monoclonal antibody to EF5 (14). Stained sections were then mounted with Vectashield (Vector Laboratories Inc., Burlingame, CA), viewed on a Zeiss microscope through immersion lens and then photographed.

For the vessel detection, the sections were incubated for 90 min with rat antimouse CD31 (platelet/endothelial cell adhesion molecule 1) monoclonal antibody (1:100; Becton Dickinson, Le Pont de Claix, France). Secondary polymer from the Envision kit (Dako, Trappes, France) was applied for 30 min at room temperature. Visualization of CD31 was realized by diaminobenzidine substrate. After rinsing in water, slides were lightly counterstained with hematoxylin. Stained sections were then mounted with Vectashield (Vector Laboratories Inc., Burlingame, CA), viewed on a Zeiss microscope through immersion lens and then photographed. The density of the vessel staining was determined using the Qwin software (Leica, Rueil-Malmaison, France) by quantifying the ratio of the anti-CD31 stained surface *versus* the total surface of the slice. Quantification was performed on at least three different xenografts in each group of treatment. Five fields were randomly chosen in each slice.

Analysis of HIF-1α Expression. Immunohistochemistry was performed on frozen tissue sections (5 μm) using Dako Ark animal research kit (Dako, Trappes, France) following manufacturer's instructions and by using a mouse antihuman HIF-1 α antibody (Becton Dickinson, Le Pont de Claix, France) at 2.5 μg/ml. The staining intensity was performed using the Qwin software by quantifying the ratio of the anti-HIF-1α stained surface *versus* the total surface of the slice after having chosen a threshold. Quantification was performed on at least three different xenografts in each group of treatment. Five fields were randomly chosen in each slice.

For the *in vitro* analysis of R115777 effect on HIF-1α expression, cells were submitted to hypoxic conditions for 4 h then treated with various concentrations of R115777 (from 0 to 7 nM) or vehicle for 4 days while maintained in hypoxic conditions. Western blotting was realized as already described (17) by using a polyclonal antihuman HIF-1α antibody (Santa-Cruz Technology; 1:500).

Analysis of MMP2 Expression and Activity. Immunohistochemistry was performed on frozen tissue sections (5 μm) fixed in 4% paraformaldehyde for 1 h and then rinsed. An endogenous peroxidase block was applied for 15 min. For MMP2 staining, the sections were incubated for 90 min at room temperature with 2 μg/ml of anti MMP2 monoclonal antibody (R&D Systems, Abingdon, United Kingdom). Secondary polymer from the Envision kit was applied for 30 min at room temperature. Visualization of MMP2 was realized by diaminobenzidine substrate. Slices were lightly counterstained with hematoxylin. Stained sections were then mounted with Vectashield (Vector Laboratories Inc.).

To perform gelatin zymography, fibronectin (Sigma) was diluted in PBS at 100 μg/ml plated, then incubated overnight at 4°C. U87 cells resuspended in serum-free DMEM, were plated

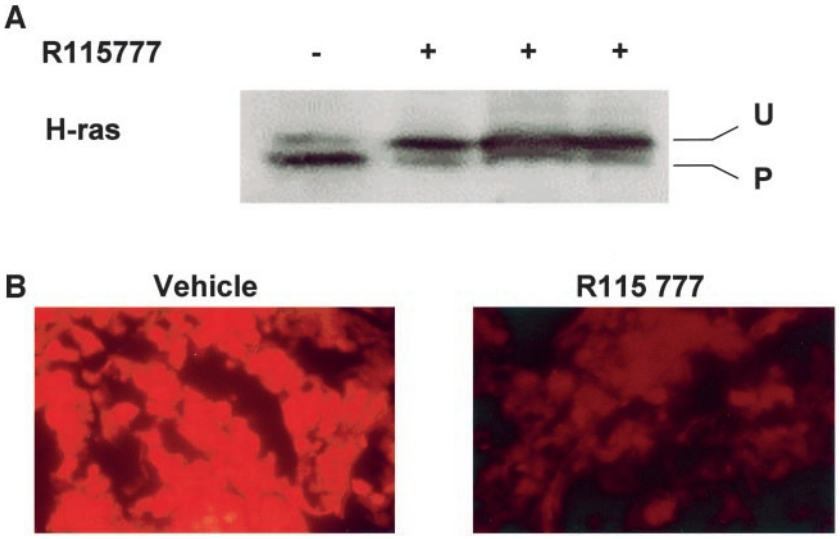

Fig. 1 *In vivo* R115777 treatment reduces hypoxia in U87 xenografts. *A*, mice bearing U87 tumors were treated with R115777 100 mg/kg bid (three different mice +) or vehicle (−) during 4 days. Western blot was performed to detect H-Ras farnesylation inhibition as described in "Materials and Methods." *Arrows* indicate the migrating position of unprocessed (*U*) and farnesylated (*P*) H-Ras forms. *B*, U87 tumor-bearing mice were treated as described in "Materials and Methods" with vehicle or with R115777. Animals were injected with EF5, euthanized, and the study of EF5 binding was performed by immunohistochemical analysis. Binding of EF5 appears in *red*. Exposure duration for each frame is: 11 s for U87 control and 15 s for U87 after R115777 treatment. Tumor sizes: 801 mm^3 for U87 control and 917 mm^3 for U87 xenografts treated with R115777. Magnification: ×630. Data represent at least five independent experiments.

at 10^7 cells in 100-mm diameter dishes coated with fibronectin and treated during 48 h with 2 nM R115777 or vehicle and returned to the incubator. The conditioned medium was obtained from 10^7 cells, and zymography was performed as already described (20).

Statistical Analysis. Student's *t* test was used to compare the different means.

RESULTS

R115777 Induces an Oxygenation of U87 Xenografts. We analyzed the effect of R115777 on oxygenation status on wild-type *ras* expressing U87 glioblastoma xenografts. For this, we first determined the conditions of *in vivo* R115777 treatment to inhibit protein farnesylation in human glioma xenografts from U87 cells. H-Ras farnesylation was followed by analyzing the appearance of the unprocessed slowly migrating H-Ras form in xenografts using Western blot. As shown on Fig. 1*A*, the *in vivo* inhibition of H-Ras farnesylation was obtained after 4 days of treatment with 100 mg/kg bid R115777 administered by gavage. Therefore, this treatment protocol was used as the basis for additional *in vivo* studies.

One of the most sensitive methods to detect hypoxia is based on the observation that binding of nitroimidazole to cellular macromolecules occurs as a result of hypoxia-dependent bioreduction by cellular nitroreductases. In particular, EF5 immunofluorescence from tumor sections has been shown to correlate well with other established indicators of tumor oxygenation such as *in situ* pO2 measurements (1). We first compared the oxygenation status of U87 xenografts in R115777-treated mice by fluorescent antibody staining for EF5 bound to tumor cells. Whereas U87 xenografts presented large regions of hypoxia in absence of treatment, the treated tumors showed little evidence of hypoxia (Fig. 1*B*). Quantitative analysis of the hypoxia was performed by determining the exposure time necessary for obtaining the same intensity of EF5 signal on photograph. The exposure time presented a 6.84 ± 1.00 fold increase after R115777 treatment ($P < 0.001$). No significant decrease of tumor size was obtained in these conditions of treatment (mean size = 957 ± 111 mm^3 for vehicle-treated mice; 745 ± 262 mm^3 for R115777-treated mice), showing that this oxygenation effect was not due to an antiproliferative effect of R115777. Taken together, these results demonstrate that R115777 treatment decreases hypoxia of U87 xenografts.

R115777 Reduces HIF1α Intracellular Level. Because HIF-1 is an essential regulator of oxygen homeostasis, we then determined whether the R115777 oxygenation effect could be related to a regulation of HIF-1α stability. For this, we analyzed the effect of R115777 on HIF-1α level in U87 xenografts by immunohistochemistry. Treating U87 xenografts with R115777 induced a significant decrease of the HIF-1α signal (m = 8.95 ± 1.08 for the control group *versus* m = 0.83 ± 0.05 for the group treated with R155777; $P < 0.05$; Fig. 2*A*). To determine whether R115777 might directly control the HIF-1α intracellular level, we analyzed the effect of R115777 treatment on HIF-1α level in U87 cells in hypoxic conditions *in vitro*. Cells were submitted to hypoxia for 4 h to induce HIF-1α expression (data not shown), then treated with various concentrations of R115777 (from 2 nM to 7 nM, the maximum drug concentration that does not inhibit cell growth) for 4 days while maintained in a environment, as done previously for the *in vivo* experiments. As shown in Fig. 2*B*, these conditions allowed farnesylation inhibition. A decrease of HIF1-α level was obtained starting at 5 nM of R115777 (Fig. 2*B*). These results demonstrate that R115777 treatment is able to modify the regulation of HIF-1α intracellular level.

R115777 Treatment Induces a Change in the Vessel Morphology and Density. Because *in vivo* oxygenation status has been related to the distance between tumor cells and the vessels, we then compared the tissue organization in U87 xenografts after treatment with R115777 or vehicle. As shown in Fig. 3*A*, tumors cells were dispersed homogeneously in the untreated xenografts. In contrast, important pauci cellular areas and a migration of the tumor cells along the vessels were observed in U87 xenografts after R155777 treatment.

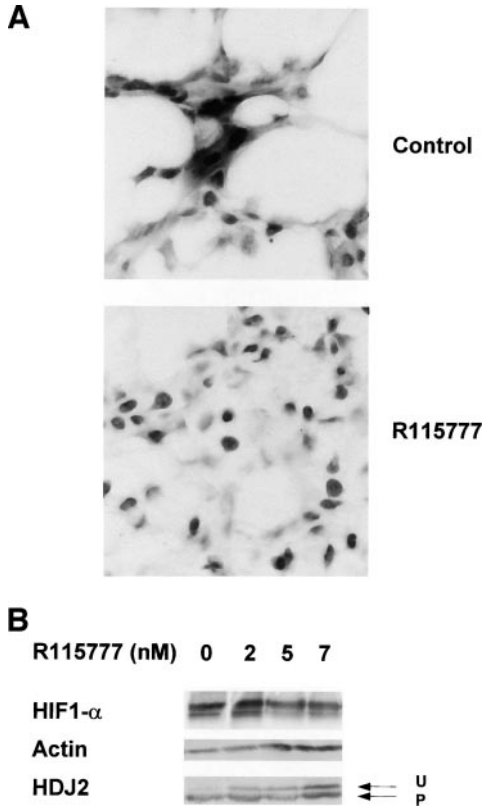

Fig. 2 R115777 treatment regulates HIF-1α intracellular level. *A,* immunohistochemistry analysis of HIF-1α was performed as described in "Materials and Methods" for U87 xenografts after treatment with vehicle or R115777. Magnification: ×400. Data represent at least three independent experiments. *B,* the amount of HIF-1α in U87 cells was analyzed by Western Blot as described in "Materials and Methods." The cells were submitted to hypoxia for 4 h, then treated with various concentrations of R115777 or vehicle for 4 days in the hypoxic condition. Western blot was performed using anti-HIF1-α antibody (*top gel*) or with anti-actin antibody (*middle gel*). Farnesylation inhibition after R115777 treatment was analyzed by performing a Western Blot using an anti-HDJ2 antibody. *Arrows* indicate the migrating position of unprocessed (*U*) and farnesylated (*P*) HDJ-2 forms (*bottom gel*). Data represent at least three independent experiments.

We then examined the vessel morphology by immunohistochemistry using anti-CD31 antibody in all of the tumors that were examined for the oxygenation status. U87 tumors showed a more heterogeneously distributed vascular network with more elongated and branched vessel structures. However, after R115777 treatment, vessel structures were more homogeneously distributed in the tumors, and the vessels appeared smaller than the vessels in the control tumors (Fig. 3*B*). Moreover, the vessel density was significantly reduced in R115777-treated xenografts compared with control xenografts ($P < 0.01$; Fig. 3*C*). These modifications in the vessel structure and the significant decrease in the vessel density strongly suggest that R115777 acts as an antiangiogenic treatment in human glioblastoma xenografts expressing wild-type ras.

R115777 Treatment Decreases MMP2 Expression and Activity. Tumor angiogenesis is regulated by different factors including enzymes implicated in proteolytic modifications of extracellular matrix, like MMPs. In human glioma, the angiogenesis and invasiveness are largely described to be linked to MMP-2 (5, 21, 22). This suggests that the antiangiogenic effect of R115777 might be mediated by MMP-2 regulation. To test whether R115777 treatment could control this pathway, we analyzed the expression of MMP2 using immunohistochemistry in U87 xenografts after treatment of the mice with R115777 or vehicle. As shown in Fig. 4*A*, the treatment of mice with R115777 induced an evident decrease of MMP2 expression in U87 xenografts. Moreover, *in vitro* study of MMP2 activity in U87 cells revealed that R115777 treatment induced a decrease of MMP2 activity (Fig. 4*B*). These data strongly suggest that a farnesylated protein regulates angiogenesis at least through the

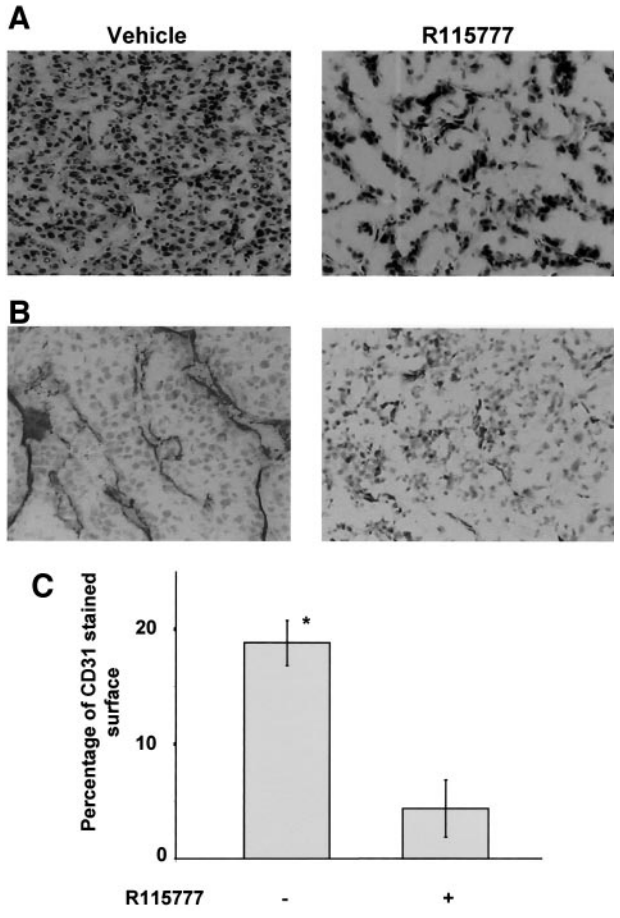

Fig. 3 R115777 treatment induces change in tumor cell organization, vessel morphology, and decreases the vessel density. *A,* cells were labeled by henalun and eosine to analyze the cell organization in U87 xenografts from mice treated or not with R115777. Magnification: ×200. Data represent at least three independent experiments *B,*. U87 tumor-bearing mice were treated as described in "Materials and Methods" by vehicle or R115777. Immunohistochemistry using anti-CD31 was performed as described in "Materials and Methods." Magnification: ×100. Data represent at least three independent experiments. *C,* The vessel density was analyzed as described in "Materials and Methods." Data represents the mean of the percentage of CD-31 stained surface in five fields from three different xenografts in each group of treatment; *bars,* ±SD. *Star, P* < 0.01.

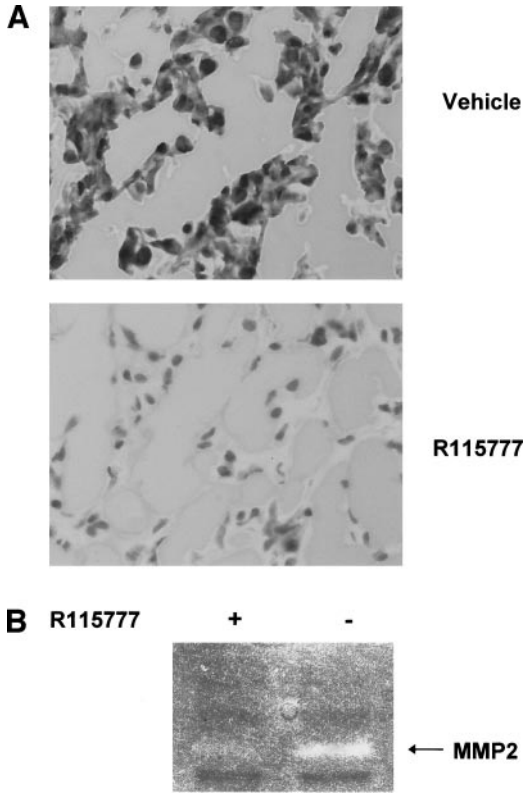

Fig. 4 R115777 treatment decreases the MMP2 expression and activity in U87tumors. *A,* immunohistochemistry analysis of MMP-2 was performed as described in "Materials and Methods" for U87 xenografts after treatment with vehicle or R115777. Magnification: ×400. Data represent at least three independent experiments. *B,* the activity of MMP-2 was analyzed by zymography as described in "Materials and Methods" in U87 cells after treatment or not with R115777. Data represent at least three independent experiments.

regulation of MMP2 expression and activity in certain human tumors like glioma.

DISCUSSION

We demonstrate here for the first time that treating human glioblastoma xenografts expressing wild-type Ras with the specific FTI, R115777, dramatically reduces the hypoxia of these tumors. Our studies have shown previously that this class of compounds is also able to increase the *in vitro* radiosensitivity of human cell lines that express wild-type Ras. We reported previously that treating M_r 24,000 FGF-2 expressing radioresistant HeLa cells with FTI induced a radiosensitization due to the inhibition by this compound of the postmitotic cell death (16). In human U87 glioblastoma cell line, R115777 treatment leads to a significant decrease in radioresistance (17). The *in vivo* oxygenation effect of FTI treatment has been demonstrated recently for tumors expressing a mutated Ras (T24 bladder carcinoma and the 141–1 murine prostate carcinoma) without any modification of two human carcinoma cell lines expressing a wild-type Ras (HT-29 from colon and RT-4 from bladder carcinoma; Ref. 12). However, these two cell lines have been radiosensitized by FTI neither *in vitro* (14) nor *in vivo* (12). These data and our results supported the hypothesis that FTI could only regulate the oxygenation of cells that are also radiosensitized by this treatment. They also suggest that a farnesylated protein other than Ras controls the oxygenation pathways in FGF-2-expressing tumors, in particular human glioblastoma.

HIF-1 is an essential regulator of oxygen homeostasis. At normal oxygen levels, the intracellular level of HIF-1 is regulated by a degradation by the ubiquitin proteasome system. Under hypoxic condition, HIF-1α is not recognized by this system, and accumulates. HIF-1 activates its target genes like VEGF, erythropoietin, glucose transport, and glycolysis genes by interacting with hypoxia-responsive elements. Our results demonstrated that R115777 treatment induced a decrease in HIF-1α level in tumor U87 xenografts *in vivo* and *in vitro* in U87 cells. This demonstrates that in Ras wild-type expressing cells, a farnesylated protein controls cellular hypoxia by regulating HIF-1α intracellular level. Because *in vivo* hypoxia could also be the result of a change in tumor vessels, we then examined the effect of R115777 on tumor vasculature. We demonstrate here that R115777 treatment promotes the migration of the tumor cells along the vessels *in vivo* and induces a more homogeneous distribution of the vessels in the tumor. Moreover, R115777 treatment significantly decreases the vessel density. This effect can explain in part the increase of the oxygenation induced by FTI treatment. In our experimental conditions, this antiangiogenic effect of R155777 did not lead to the decrease of tumor growth. Treating mice for 4 days was certainly not long enough to induce a significant change in tumor size even if we can observe a modification of the hypoxia and the vasculature. These combined effects on vasculature and oxygenation have been observed with antiangiogenic agents such as AGM-1470 (23), antibodies to VEGF (24), or suramin (25) in human glioblastoma xenografts. The potential antiangiogenic effect of FTI has already been described using several models. Gu *et al.* (26) showed that the FTI A-17063 induced a 41% decrease of the vascularization in and around a K-ras mutated colon carcinoma xenograft related to the *in vitro* decrease of VEGF. A recent study showed that treatment with the FTI B1620 of mice bearing U87 xenografts resulted in a significant decrease of vascularity (27). Several studies have demonstrated that treating human glioblastoma cell lines with FTI leads to the decrease of VEGF expression (28). However, angiogenesis is not only dependent on VEGF but also requires proteolytic modifications of the extracellular matrix by metalloproteinases. We then determined the effect of FTI treatment on the regulation of MMP2 in U87 xenografts and cells. We demonstrate here that the protein farnesylation inhibition induced a decrease of MMP2 expression in U87 xenografts. Moreover, treating U87 cells *in vitro* with R115777 inhibited the activity of this metalloproteinase. Inhibition of the protein prenylation by lovastatin has already been described to induce a decrease in MMP-9 but not MMP-2 activity in NIH3T3 and v-H-Ras 3T3 fibroblasts (29). In human monocytic cell lines, the inhibition of MMP-9 activity was only obtained after treatment with geranylgeranyltransferase inhibitors. Our results demonstrate for the first time that a farnesylated protein could regulate angiogenesis at least through the regulation of MMP2 expression and activity in certain human tumors like glioma. Among the farnesylated proteins known to be involved in the control of cellular radioresistance and microen-

vironment is Ras (13, 14, 30). However, we have shown previously that another farnesylated protein, RhoB, regulates the cellular radioresistance of wild-type Ras-expressing cells (17, 18). Our most recent results strongly suggest that in our model, RhoB might be one of the targets of R115777 for its effects on hypoxia and angiogenesis.

Taken together, our previous data and these results demonstrate that R115777 treatment is able to inhibit different mechanisms leading to poor efficiency of the standard treatment of the glioblastoma, that is to say intrinsic cellular radioresistance, hypoxia, and tumor aggressiveness. These combined effects on glioblastoma underline the interest of associating R115777 with radiotherapy as a new treatment for these catastrophic prognosis tumors.

ACKNOWLEDGMENTS

We thank Dr. Cameron Koch, University of Pennsylvania, for providing EF5 and Cy3-conjugated ELK-51.

REFERENCES

1. Nozue, M., Lee, I., Yuan, F., Teicher, B. A., Brizel, D. M., Dewhirst, M. W., Milross, C. G., Milas, L., Song, C. W., Thomas, C. D., Guichard, M., Evans, S. M., Koch, C. J., Lord, E. M., Jain, R. K., and Suit, H. D. Interlaboratory variation in oxygen tension measurement by Eppendorf "Histograph" and comparison with hypoxic marker. J. Surg. Oncol., *66:* 30–38, 1997.

2. Brizel, D. M., Sibley, G. S., Prosnitz, L. R., Scher, R. L., and Dewhirst, M. W. Tumor hypoxia adversely affects the prognosis of carcinoma of the head and neck. Int. J. Radiat. Oncol. Biol. Phys., *38:* 285–289, 1997.

3. Brizel, D. M., Scully, S. P., Harrelson, J. M., Layfield, L. J., Bean, J. M., Prosnitz, L. R., and Dewhirst, M. W. Tumor oxygenation predicts for the likelihood of distant metastases in human soft tissue sarcoma. Cancer Res., *56:* 941–943, 1996.

4. Hockel, M., Knoop, C., Schlenger, K., Vorndran, B., Knapstein, P. G., and Vaupel, P. Intratumoral pO2 histography as predictive assay in advanced cancer of the uterine cervix. Adv. Exp. Med. Biol., *345:* 445–450, 1994.

5. Uhm, J. H., Dooley, N. P., Villemure, J. G., and Yong, V. W. Glioma invasion *in vitro:* regulation by matrix metalloprotease-2 and protein kinase C. Clin. Exp. Metastasis, *14:* 421–433, 1996.

6. Barrington, R. E., Subler, M. A., Rands, E., Omer, C. A., Miller, P. J., Hundley, J. E., Koester, S. K., Troyer, D. A., Bearss, D. J., Conner, M. W., Gibbs, J. B., Hamilton, K., Koblan, K. S., Mosser, S. D., O'Neill, T. J., Schaber, M. D., Senderak, E. T., Windle, J. J., Oliff, A., and Kohl, N. E. A farnesyltransferase inhibitor induces tumor regression in transgenic mice harboring multiple oncogenic mutations by mediating alterations in both cell cycle control and apoptosis. Mol. Cell Biol., *18:* 85–92, 1998.

7. Kohl, N. E., Wilson, F. R., Mosser, S. D., Giuliani, E., deSolms, S. J., Conner, M. W., Anthony, N. J., Holtz, W. J., Gomez, R. P., and Lee, T. J. Protein farnesyltransferase inhibitors block the growth of ras-dependent tumors in nude mice. Proc. Natl. Acad. Sci. USA, *91:* 9141–9145, 1994.

8. Sun, J., Qian, Y., Hamilton, A. D., and Sebti, S. M. Ras CAAX peptidomimetic FTI 276 selectively blocks tumor growth in nude mice of a human lung carcinoma with K-Ras mutation and p53 deletion. Cancer Res., *55:* 4243–4247, 1995.

9. End, D. W., Smets, G., Todd, A. V., Applegate, T. L., Fuery, C. J., Angibaud, P., Venet, M., Sanz, G., Poignet, H., Skrzat, S., Devine, A., Wouters, W., and Bowden, C. Characterization of the antitumor effects of the selective farnesyl protein transferase inhibitor R115777 *in vivo* and *in vitro*. Cancer Res., *61:* 131–137, 2001.

10. McKenna, W. G., Iliakis, G., Weiss, M. C., Bernhard, E. J., and Muschel, R. J. Increased G_2 delay in radiation-resistant cells obtained by transformation of primary rat embryo cells with the oncogenes H-ras and v-myc. Radiat. Res., *125:* 283–287, 1991.

11. McKenna, W. G., Weiss, M. C., Bakanauskas, V. J., Sandler, H., Kelsten, M. L., Biaglow, J., Tuttle, S. W., Endlich, B., Ling, C. C., and Muschel, R. J. The role of the H-ras oncogene in radiation resistance and metastasis. Int. J. Radiat. Oncol. Biol. Phys., *18:* 849–859, 1990.

12. Cohen-Jonathan, E., Muschel, R. J., Gillies, M. W., Evans, S. M., Cerniglia, G., Mick, R., Kusewitt, D., Sebti, S. M., Hamilton, A. D., Oliff, A., Kohl, N., Gibbs, J. B., and Bernhard, E. J. Farnesyltransferase inhibitors potentiate the antitumor effect of radiation on a human tumor xenograft expressing activated HRAS. Radiat. Res., *154:* 125–132, 2000.

13. Bernhard, E. J., Kao, G., Cox, A. D., Sebti, S. M., Hamilton, A. D., Muschel, R. J., and McKenna, W. G. The farnesyltransferase inhibitor FTI-277 radiosensitizes H-ras-transformed rat embryo fibroblasts. Cancer Res., *56:* 1727–1730, 1996.

14. Bernhard, E. J., McKenna, W. G., Hamilton, A. D., Sebti, S. M., Qian, Y., Wu, J. M., and Muschel, R. J. Inhibiting Ras prenylation increases the radiosensitivity of human tumor cell lines with activating mutations of ras oncogenes. Cancer Res., *58:* 1754–1761, 1998.

15. Cohen-Jonathan, E., Evans, S. M., Koch, C. J., Muschel, R. J., McKenna, W. G., Wu, J., and Bernhard, E. J. The farnesyltransferase inhibitor L744, 832 reduces hypoxia in tumors expressing activated H-ras. Cancer Res., *61:* 2289–2293, 2001.

16. Cohen-Jonathan, E., Toulas, C., Ader, I., Monteil, S., Allal, C., Bonnet, J., Hamilton, A. D., Sebti, S. M., Daly-Schveitzer, N., and Favre, G. The farnesyltransferase inhibitor FTI-277 suppresses the 24-kDa FGF2-induced radioresistance in HeLa cells expressing wild-type RAS. Radiat. Res., *152:* 404–411, 1999.

17. Delmas, C., Heliez, C., Cohen-Jonathan, E., End, D., Bonnet, J., Favre, G., and Toulas, C. Farnesyltransferase inhibitor, R115777, reverses the resistance of human glioma cell lines to ionizing radiation. Int. J. Cancer, *100:* 43–48, 2002.

18. Ader, I., Toulas, C., Dalenc, F., Delmas, C., Bonnet, J., Cohen-Jonathan, E., and Favre, G. RhoB controls the 24 kDa FGF-2-induced radioresistance in HeLa cells by preventing post-mitotic cell death. Oncogene, *21:* 5998–6006, 2002.

19. Dalenc, F., Drouet, J., Ader, I., Delmas, C., Rochaix, P., Favre, G., Cohen-Jonathan, E., and Toulas, C. Increased expression of a COOH-truncated nucleophosmin resulting from alternative splicing is associated with cellular resistance to ionizing radiation in HeLa cells. Int. J. Cancer, *100:* 662–668, 2002.

20. Deb, S., Zhang, J. W., and Gottschall, P. E. Activated isoforms of MMP-2 are induced in U87 human glioma cells in response to β-amyloid peptide. J. Neurosci. Res., *55:* 44–53, 1999.

21. Bello, L., Lucini, V., Carrabba, G., Giussani, C., Machluf, M., Pluderi, M., Nikas, D., Zhang, J., Tomei, G., Villani, R. M., Carroll, R. S., Bikfalvi, A., and Black, P. M. Simultaneous inhibition of glioma angiogenesis, cell proliferation, and invasion by a naturally occurring fragment of human metalloproteinase-2. Cancer Res., *61:* 8730–8736, 2001.

22. Gingras, D., Page, M., Annabi, B., and Beliveau, R. Rapid activation of matrix metalloproteinase-2 by glioma cells occurs through a posttranslational MT1-MMP-dependent mechanism. Biochim. Biophys. Acta, *1497:* 341–350, 2000.

23. Bernsen, H. J., Rijken, P. F., Peters, H., Bakker, H., and van der Kogel, A. J. The effect of the anti-angiogenic agent TNP-470 on tumor growth and vascularity in low passaged xenografts of human gliomas in nude mice. J. Neurooncol., *38:* 51–57, 1998.

24. Kim, K. J., Li, B., Winer, J., Armanini, M., Gillett, N., Phillips, H. S., and Ferrara, N. Inhibition of vascular endothelial growth factor-induced angiogenesis suppresses tumour growth *in vivo*. Nature (Lond.), *362:* 841–844, 1993.

25. Bernsen, H. J., Rijken, P. F., Peters, J. P., Bakker, J. H., Boerman, R. H., Wesseling, P., and van der Kogel, A. J. Suramin treatment of human glioma xenografts; effects on tumor vasculature and oxygenation status. J. Neurooncol., *44:* 129–136, 1999.

26. Gu, W. Z., Tahir, S. K., Wang, Y. C., Zhang, H. C., Cherian, S. P., O'Connor, S., Leal, J. A., Rosenberg, S. H., and Ng, S. C. Effect of novel CAAX peptidomimetic farnesyltransferase inhibitor on angiogenesis *in vitro* and *in vivo*. Eur. J. Cancer, *35:* 1394–1401, 1999.

27. Kurimoto, M., Hirashima, Y., Hamada, H., Kamiyama, H., Nagai, S., Hayashi, N., and Endo, S. *In vitro* and *in vivo* growth inhibition of human malignant astrocytoma cells by the farnesyltransferase inhibitor B1620. J. Neurooncol., *61:* 103–112, 2003.

28. Feldkamp, M. M., Lau, N., and Guha, A. Growth inhibition of astrocytoma cells by farnesyl transferase inhibitors is mediated by a combination of anti-proliferative, pro-apoptotic and anti-angiogenic effects. Oncogene, *18:* 7514–7526, 1999.

29. Wang, I. K., Lin-Shiau, S. Y., and Lin, J. K. Suppression of invasion and MMP-9 expression in NIH 3T3 and v-H-Ras 3T3 fibroblasts by lovastatin through inhibition of ras isoprenylation. Oncology, *59:* 245–254, 2000.

30. Mazure, N. M., Chen, E. Y., Laderoute, K. R., and Giaccia, A. J. Induction of vascular endothelial growth factor by hypoxia is modulated by a phosphatidylinositol 3-kinase/Akt signaling pathway in Ha-ras-transformed cells through a hypoxia inducible factor-1 transcriptional element. Blood, *90:* 3322–3331, 1997.